Proceedings of ASME Turbo Expo 2011
GT2011
June 6-10, 2011, Vancouver, British Columbia, Canada

GT2011-45583

INCREASING THE PASSIVE SCALAR MIXING QUALITY OF JETS IN CROSSFLOW WITH FLUIDICS ACTUATORS

Arnaud Lacarelle[*]
Christian O. Paschereit
Institut für Strömungsmechanik und Technische Akustik
Technische Universität Berlin
Berlin, Germany

ABSTRACT

Jets in crossflow are widely used in the industry for homogenization or cooling tasks. Recently, pulsating jets have been investigated as a mean to increase the scalar mixing efficiency of such configurations, whether for a single jet or for an array of jets. To avoid the disadvantages of mechanically actuated flows (costs, maintenance), a new injector based on a fluidics oscillator has been designed. Four injectors have been implemented in a generical jet in crossflow configuration and the mixing efficiency of the setup was compared with the one of the same setup equiped with standard non oscillating jets. With help of high-speed concentration measurement technique, the scalar mixing quality of both setups was measured at three positions downstream of the injection plane.

In all the cases tested, the fluidics injectors present a better temporal homogenization, characterized with the Danckwerts unmixedness criterion, than the standard jets. For a defined mixing quality, a decrease of the mixing length by approximately 50% can be achieved with the fluidics injectors. Furthermore, the new injectors exhibit a mixing quality which is less sensitive to variations of the jet to crossflow momentum. The flapping motion of the fluidics injectors induces a wider azimuthal spreading of the fluidics jets immediately downstream of the injection location. This increases the macro- and micromixing phenomea which lead then to the high gains in mixing quality. It is thus demonstrated that fluidics oscillators present a strong potential to improve the passive scalar homogenization of jet in crossflow configurations.

NOMENCLATURE

C Volumetric concentration of dye
C^* Normalized volumetric concentration of dye
D Burner diameter
d_h Jet exit hydraulic diameter
J Jet to crossflow momentum ratio
PDF Probability Density Function
Re Reynolds number
St Strouhal number
σ Standard deviation of concentration fluctuations
U_t Danckwerts temporal unmixedness
U_x Danckwerts spatial unmixedness
w_0 Main channel bulk velocity
w_j Jet bulk velocity
x Axial position

INTRODUCTION

Controlling the mixing of two or more components is still an important and challenging task in current industrial systems. For example, the control of the fuel/air mixing in aero-engines or heavy duty turbines, is critical regarding pollutant emissions or flame stabilization. The control of secondary air injections is also relevant for cooling considerations. The chemical industry is also very interested in rapidly and/or efficiently mixing reactants.

[*]Address all correspondence to this author, arnaud.lacarelle@tu-berlin.de.

One of the simplest and most effective way of mixing two fluids together is to use a jet in crossflow injection, where one of the fluids is injected into the second one with an angle generally close to 90°. With increasing downstream distance, the degree of homogenization increases, and a minimal mixing length has to be set to achieve a defined degree of homogenization. As the decay of the unmixedness (typically a normalized expression of the variance of the concentration fluctuations) along the mixing path x can be roughly approximated with a $1/x$ function, a decrease of the unmixedness by a factor two will require a mixing path two times longer, increasing the costs and weight of the installation considered. This justifies the need to mix more rapidly different fluids in crossflow configurations.

The first works characterizing the mixing of crossflow jets focussed on passive modification of the system geometry. Experimental and numerical studies of simple jets in a fluid at rest presented in the review of Gutmark and Grinsten [1] showed that the mean and coherent flow fields are strongly affected by the jet exit shape. In particular, the use of tabs at the exit of a jet was shown to greatly increase the entrainment mass flow compared to the reference jet without tabs. It is thus expected that the mixing quality would improve due to a greater macro homogenization. Unfortunately, no measurements of scalar mixing quality are reported. Instead, these flow field changes seem to marginaly affect the passive scalar mixing proces in jets in crossflows. In particular the work of Liscinsky et al. [2] evidences that a change in the jet exit shape, the use of tabs at the outlet, or the use of a swirl upstream of the jet exit, lead only to marginal changes in the mixing quality recorded in the near field of a jet in crossflow.

The small effect of such passive jet modifications motivated the work on active control methods. The works of Johari [3, 4] or Eroglu and Breidenthal [5] showed that it is indeed possible to influence strongly the mixing of a jet in crossflow when the jet is modulated with a square wave. Depending on the parameters set (frequency, signal shape, amplitude, duty-cycle) different flow regimes occur. The best mixing qualities are obtained when distinct vortex rings are created to ensure a strong penetration and dilution. The mixing quality shows in any case a strong dependence on the parameter sets. Investigations performed by Lacarelle et al. [6] also demonstrated the potential of a square actuation to increase the small-scale mixing at the outlet of a premixed burner.

The studies [3–6] had the particularity of being performed in water. Recent LES simulations on a gaseous pulsed jet in crossflow performed by Coussement et al. [7] somehow dampened the previous experimental results, as they reported in the near field an increase of the overall mixing quality with a sinusoidal wave and not with a pulsed signal. A direct comparison with the previous work is not possible, but the question of the transfer of aqueous results into gaseous flows is at least open.

One drawback of active pulsation is the use of mechanical valve to actuate the main jet. A large frequency band width is generally required to achieve the optimal injection conditions for a required total mass flow (superior to 200 Hz in the air). Therefore methods which circumvent the use of mechanical actuator are required. Fluidics actuators, which are self-oscillating flow devices, are suitable to fulfill these needs. Nathan et al. [8] offered an extensive description of the effects of such self-oscillating devices on the velocity and passive scalar fields recorded downstream of the injection location. They show in particular that the increase of the mixing quality is higher in the near field of the injector than in the far field. Hence, the use of fluidics actuators will depend on how fast the mixing must occur in a technical application. If short mixing lengths are required, they are expected to bring non-negligible gains compared to standard and non-oscillating injectors.

In the upcoming sections, the mixing efficiency of fluidics injectors is compared with the one of standard jets with an identical outlet geometry. The statistical analysis of the concentration measurements present clearly the advantages of fluidics injectors for the different operating conditions tested.

EXPERIMENTAL SETUP AND MEASUREMENT TECHNIQUES

The investigated setup is a generic jet in crossflow configuration; a lance is mounted centered in a square channel of side length L. Through four rectangular holes a mixture of fluorescent dye and water is injected with an angle of 90° relative to the main water flow. The main direction of the dye injection is colinear to the diagonal of the cross-section of the square channel as illustrated in Fig. 1.

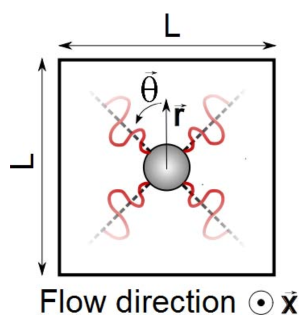

Figure 1. JET IN CROSSFLOW CONFIGURATION AND ILLUSTRATION OF THE FLUIDICS OSCILLATION PLANE

Two types of injectors are considered in this study; a standard jet and a fluidics jet. Both jets have the same rectangular outlet corresponding to a hydraulic diameter d_h. The ratio of the sides of the rectangle is equal to 2.35 and the longest side is parallel to the main flow direction. The fluidics injectors induce an azimuthal jet oscillation in a plane perpendicular to the direction of the main flow. This oscillation is expected to increase the dilution of the jet with the surrounding fluid by increasing first the macro-mixing (i.e. the spatial distribution of the fuel) close to the injection and then the micromixing, as the surface of contact between the dye and the main flow is expected to augment when compared to a standard jet injection.

A sketch of the type of fluidics investigated is presented in Fig. 2. It is similar to the one used by Guyot et al. [9] which was successfully implemented to control the thermoacoustic instabilities of a combustion chamber. The main difference is that the present design has only one outlet port instead of two. Furthermore the actuator was downscaled by a factor close to 1/10 to fit in the geometrical constraints of the system tested. Design and manufacturing were performed by Advanced Fluidics Corporation.

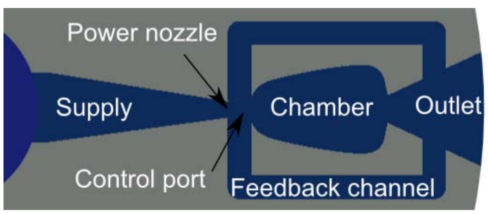

Figure 2. SIMPLIFIED SKETCH OF THE FLUIDICS INJECTOR

The steady flow enters the fluidics through the power nozzle and is converted in a planar oscillating flow through the combination of flow attachment in the chamber and alternating feedback of the two feedback channels (for a more extensive description cf. [9]). The resulting flapping motion of the jet at the outlet is illustrated over one period in Fig. 3. In particular the 4. and 7. pictures, which are taken close to the maximal injection angles of the fluidics, illustrate the wide azimuthal region covered by the jet.

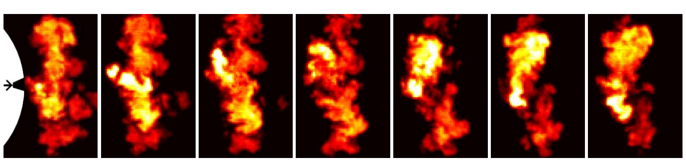

Figure 3. ONE PERIOD OF OSCILLATION OF THE FLUIDICS INJECTOR RECORDED AT x/d_h=2.2

The major impact of downsizing the fluidics is an increase of the oscillation frequency at a constant volume flow as the feedback time constant depends on the mean velocity in the feedback channels. The frequencies involved in the air with the present fluidics would be typically of the order of 1000 Hz (not measured here). In water, they were of the order of 20 Hz and higher.

The tests are performed in a water test rig and the test section is illustrated in Fig. 4. Three screens placed upstream of the injection location ensure a symmetrical velocity profile of the main flow. The Reynolds number in the square test section is calculated as

$$Re = \frac{w_0 D_h}{\nu}, \tag{1}$$

where D_h is the hydraulic diameter of the cross-section area of size $L \times L$, w_0 the mean bulk velocity of the test section and ν the water viscosity. In the present work, the Reynold number was set at Re=72300, which is high enough to ensure a relative independency of the mixing process with an increase of the mean bulk velocity.

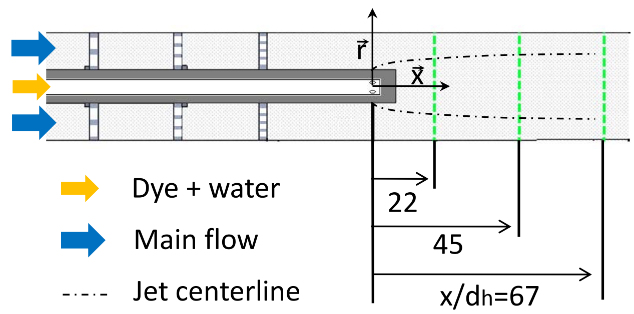

Figure 4. SLICE OF THE TEST CHANNEL AND LOCALIZATION OF THE AXIAL MEASUREMENT PLANES DOWNSTREAM OF THE INJECTION LOCATION

A second critical parameter for the mixing process is the jet to crossflow momentum ratio which is calculated as the squared ratio of the jet bulk velocity w_j to the main flow bulk velocity w_0 and reads

$$J = \left(\frac{w_j}{w_0}\right)^2. \tag{2}$$

In the present work, J is equal to 2.3, 6.4, 17.7, or 55.

The concentrations are recorded with high-speed laser-induced fluorescence (HSLIF). A high-speed camera (Photron Fastcam PCI 1024) records at a frame rate of 125 Hz or 250 Hz the mixing process in the axial planes shown in Fig. 4. A 4 Watt continuous wave laser with a wavelength of 532 nm generates a δ_L = 0.5 mm thick laser sheet and excites the rhodamine 6G present in the jet flow. The average particle displacement δ_s

in the flow direction due to the camera shutter time verifies $\delta_s \approx 0.5\delta_L$. This value is small enough to consider the recorded pictures as a frozen pattern of the mixing process.

The calibration and correction of the mixing snapshots is typical for laser-induced fluorescence measurements. A background picture (average picture taken without dye) is subtracted from the recorded pictures, giving the background corrected pictures. An average picture of known homogeneous dye concentration is then recorded and background corrected. Under the assumption of linear fluorescence response, the real local concentrations are easily obtained from the ratio of the background corrected snapshots to the homogeneous and background corrected average picture. However, as a relatively high homogeneous concentration is needed to obtain a good camera signal, resulting partly in a non-linear response, the dye absorption had to be taken into account. This was done using the absorption law of Beer. More details on the correction method can be taken from [6]. Finally, all the concentrations are normalized between 0 and 1 with the reference concentration of the unmixed fuel injection, i.e. $C_0 = 3.17 \times 10^{-6}$ mol/l. The resulting concentrations are then dimensionless and noted C^*, the star symbol indicating the dimensionless expression.

To compare the mixing effectiveness of the considered injectors, the spatial and temporal unmixedness criteria based on the definition of the intensity of segregation of Danckwerts [10], U_x and U_t, are calculated. They reflect how inhomogeneous the mixture is, 0 indicating a perfect mixture and 1 a completely segregated mixture. The general definition of the unmixedness is a normalized expression of the concentration fluctuations variance which reads

$$U = \frac{\sigma^2}{\sigma_0^2} = \frac{\sigma^2}{C^*_\infty \left(1 - C^*_\infty\right)}, \tag{3}$$

where σ^2 is the mixture variance in the measurement plane and σ_0^2 the variance immediately before the start of the mixing process (i.e. independant of the measurement position). Depending on how the variance of the mixture σ^2 is calculated in Eq. 3, the spatial unmixedness U_x and the temporal unmixedness U_t are calculated. $U_x = \sigma_x^2/\sigma_0^2$ is obtained from the variance σ_x^2 of the temporally averaged concentration field $\overline{C^*}(i)$ recorded by the N_i pixels of the camera and which reads

$$\sigma_x^2 = \frac{1}{N_i - 1} \sum_{i=1}^{N_i} \left(\overline{C^*}(i) - C^*_\infty\right)^2, \tag{4}$$

C^*_∞ being the concentration of the ideally mixed mixture. i is the index of the camera pixels. U_x can be considered as a measure of the macro-mixing and answers the question how good the two fluids are *in average* spatially mixed in the measurement plane. Temporal fluctuations, which typically dominate the mixing processes, are thus not taken into account. This is done by the parameter $U_t = \sigma_t^2/\sigma_0^2$ in which the variance σ_t^2 of all the concentrations recorded by the pixels of the camera is calculated as

$$\sigma_t^2 = \frac{1}{N_i N_t - 1} \sum_{i=1}^{N_i} \sum_{t=1}^{N_t} \left(C^*(i,t) - C^*_\infty\right)^2, \tag{5}$$

where N_t corresponds to the numer of snapshots recorded during one mixing run. U_t is more approriate to describe the mixing quality of technical systems as the spatial unmixedness is not able to capture temporal concentration fluctuations. However, both criteria together give a better understanding of the mixing mechanisms and are thus reported in the present work.

INSTANTANEOUS MIXING AND FLUIDICS OSCILLATION FREQUENCY

Instantaneous concentration

Before performing any statistical post-processing of the pictures, the instantaneous snapshots of the mixing processes at x/d_h=67 show in Fig. 5 illustrate clearly the differences between standard jet and fluidics mixing. The structure of the concentration distribution greatly changes between the fluidics and the reference injectors; the fluidics injectors present a more homogenized and central pattern than the reference injection, which presents four distinct islands. The maximal concentrations encountered are also lower in the fluidics case, indicating a better dilution of the fuel with the surroundings. These snapshots are thus qualitatively indicating that the mixing quality increases when the fluidics injectors are used. Similar conclusions could be drawn for instantaneous snapshots recorded in the two other measurement planes.

Fluidics frequency

The frequency of the fluidics oscillation was calculated from the FFT analysis of local concentration fluctuations recorded at a distance $x/d_h = 2.2$ downstream of the fuel injection location. The measurements were performed for different dye mass flows and hence different jet Reynolds numbers. The main volume flow was set at a very low value simply to avoid the accumulation of dye in the measurement plane. Figure 6 depicts the evolution of the normalized frequency (Strouhal number based on the hydraulic diameter of the rectangular injector, St=$f d_h/w_j$) of the fluidics with the jet Reynolds number.

A small decrease of the Strouhal number (from 0.07 down to 0.05) is visible with an increasing jet Reynolds number. This means that the frequency of the jet oscillation is not a linear function of the velocity. Regarding the present work and a constant

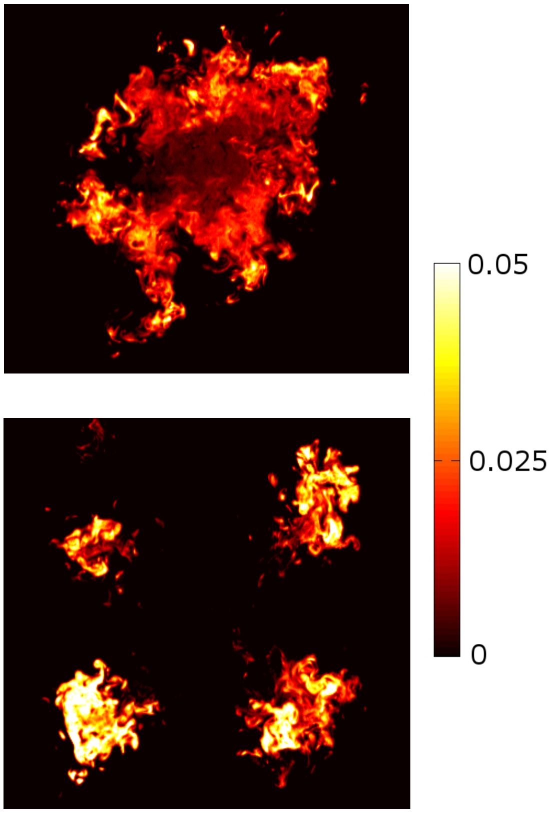

Figure 5. INSTANTANEOUS CONCENTRATIONS RECORDED AT THE MEASUREMENT PLANE $x/d_h = 67$. TOP: FLUIDICS INJECTION, BOTTOM: STANDARD INJECTION. $Re = 72300$, $J = 17.7$.

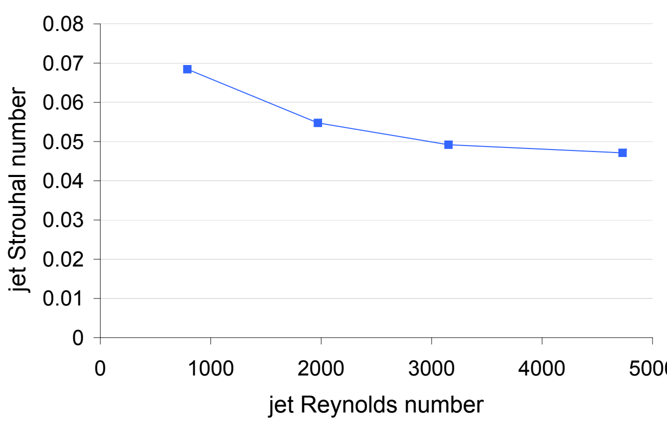

Figure 6. FLUIDICS STROUHAL NUMBER (St=fd_h/w_j) DEPENDING ON THE JET REYNOLDS NUMBER OF THE FUEL INJECTION

main flow Reynolds number, this means also that an increase of the jet to crossflow momentum will induce an increase of the oscillation frequency. This frequency change may certainly also affect the mixing process. However, the variation of one parameter at once (frequency or jet momentum) would have required hardware modifications to adjust the oscillation frequency. This was not performed in the present work, as it is not relevant for practical applications where one fluidics geometry should work well for different operating conditions. The reader should thus bear in mind when looking at the following charts that an increase of the jet momentum is linked with an increase of the fluidics oscillation frequency.

MIXING COMPARISON AT ONE AXIAL LOCATION

The average and RMS concentrations in the measurement plane $x/d_h = 67$ for the jet to crossflow momentum $J = 17.7$ are presented first in the following section.

Average concentration

The comparison of the average concentrations confirms the first impressions gained from the instantaneous pictures: the dye distribution of the fluidics injectors is more concentrated in the center of the square channel while 4 distinct islands are visible for the standard injectors. Even if the injector geometry ensures an equal mean bulk velocity at the outlet of the injectors (and hence an identical absolute jet to crossflow momentum), it is clear that the oscillating motion leads to a much lower penetration of the fluidics injector. This low jet penetration is responsble for the centered pattern.

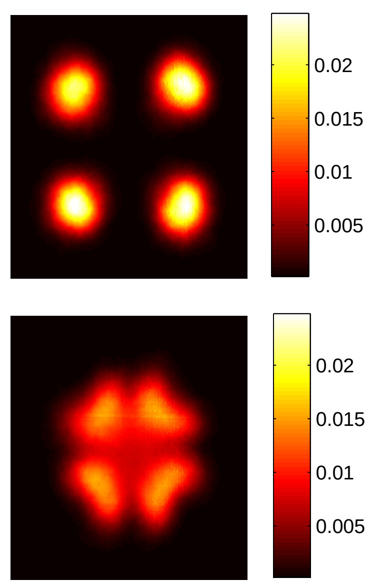

Figure 7. AVERAGE CONCENTRATION PICTURES FOR THE STANDARD (TOP) AND FLUIDICS (BOTTOM) INJECTIONS, RECORDED AT $x/d_h = 67$, $J = 17.7$.

Furthermore, the maximal locally averaged concentrations are slightly lower for the fluidics injection than for the reference jet in crossflow. This result is well illustrated by the probability density functions of the temporally averaged concentration shown in Fig. 8: the maximal average concentration of the reference case is close to $\overline{C^*}$ =0.025 while the fluidics case shows a much lower maximal concentration of $\overline{C^*}$ =0.015. This confirms that the dilution of the fluidics jet with the surrounding flow is much higher than the one of the standard crossflow jet.

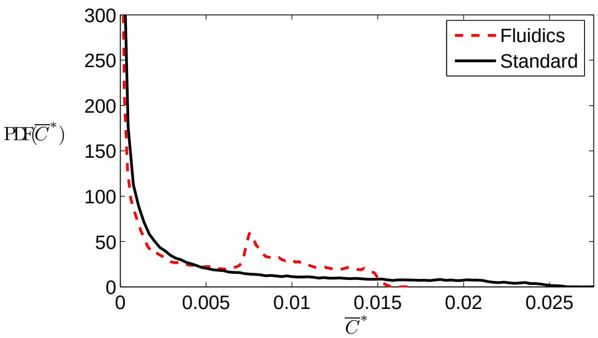

Figure 8. COMPARISON OF THE PROBABILITY DENSITY FUNCTIONS OF THE TIME AVERAGED CONCENTRATION FOR THE STANDARD AND THE FLUIDICS INJECTIONS, RECORDED AT $x/d_h = 67$, $J = 17.7$

Concentration fluctuations

The improvement of the mixing is also visible in the pictures of the RMS values of the concentration fluctuations. The images shown in Fig. 9 present first a pattern similar to the average concentration pictures shown in the previous section. This is particularly true for the standard jet injection. For the fluidics injection, the position of the maxima in concentration fluctuations are slightly shifted radially when compared to the maxima of the temporally averaged concentration pictures (Fig. 7).

The amplitude of the concentration fluctuations is also much lower with the fluidics injection than with the standard jet injection, as confirmed by the PDF of the two injection types shown in Fig. 10. This decrease of the local concentration fluctuations is an indication of an increase in the micro-mixing quality.

MIXING QUALITY IMPROVEMENT

Evolution of the unmixedness parameters at x/d_h=22 and x/d_h=112

The spatial and temporal unmixedness criteria allow for quantifying the mixing quality. Looking at the results recorded at x/d_h=22 downstream of the injection location (Fig. 11), the

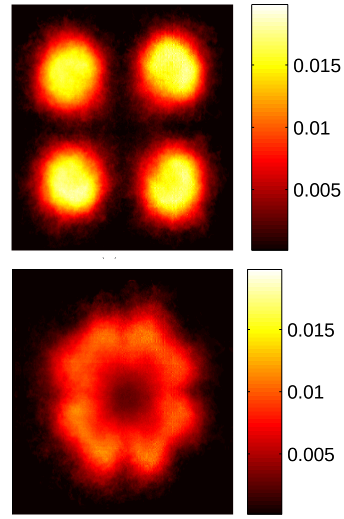

Figure 9. RMS CONCENTRATION PICTURES FOR THE STANDARD (TOP) AND FLUIDICS (BOTTOM) INJECTIONS, RECORDED AT $x/d_h = 67$, $J = 17.7$.

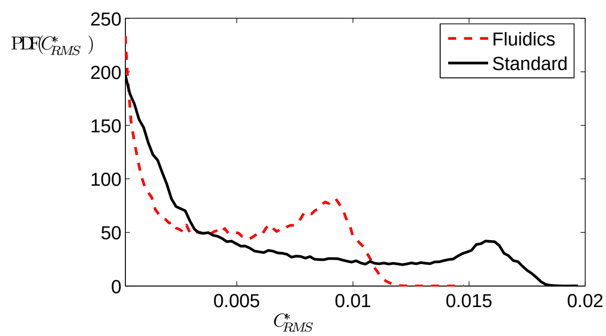

Figure 10. COMPARISON OF THE PROBABILITY DENSITY FUNCTIONS OF THE RMS CONCENTRATION FOR THE STANDARD AND THE FLUIDICS INJECTIONS, RECORDED AT $x/d_h = 67$, $J = 17.7$

fluidics injectors present a dramatic enhancement of the mixing quality when compared to the standard injection: a decrease by approximately 50% of the spatial unmixedness U_x and of the temporal unmixedness U_t are recorded. Even if less pronounced, the gain in mixing quality at $x/d_h = 112$ can still reach 50% if the momentum ratio is properly adjusted (J=17.7 in Fig. 12).

Furthermore, for the fluidics injector and the two illustrated measurement planes, the mixing quality is mostly independent of the injection momentum J, while the standard injection presents stronger variations. These results may be of strong importance if different operating points involving different momentum ratios are used in the practical application. The fluidics injectors would ensure a constant mixing quality over the different operating con-

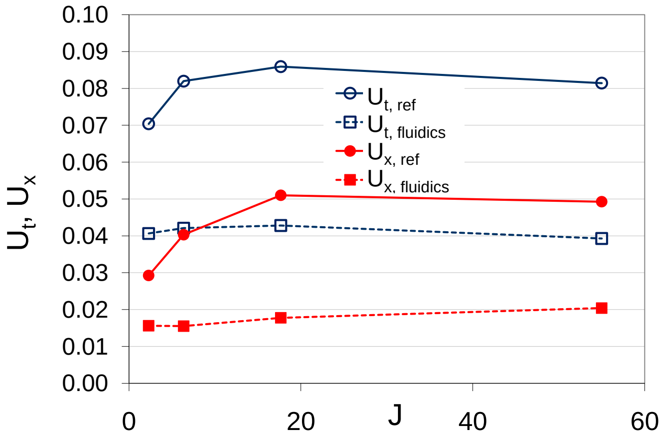

Figure 11. SPATIAL AND TEMPORAL UNMIXEDNESS CRITERIA DEPENDING ON THE JET TO CROSSFLOW MOMENTUM RECORDED AT $x/d_h = 22$

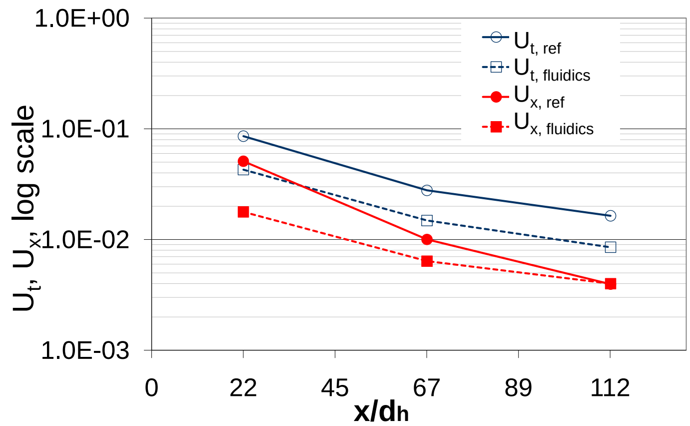

Figure 13. SPATIAL AND TEMPORAL UNMIXEDNESS CRITERIA DEPENDING ON THE STREAMWISE LOCATION FOR J=17.7

ditions.

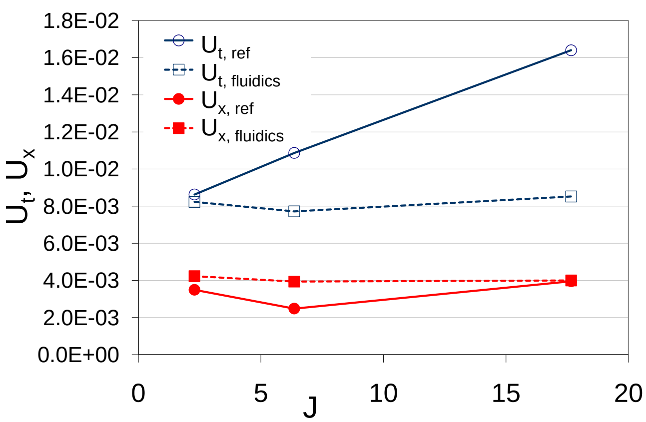

Figure 12. SPATIAL AND TEMPORAL UNMIXEDNESS CRITERIA DEPENDING ON THE JET TO CROSSFLOW MOMENTUM RECORDED AT $x/d_h = 112$

Axial evolution of U_x and U_t for J=17.7

The same data were plotted over the mixing length x/d_h and are shown in Fig. 13. It confirms that the fluidics injector presents a better macro-mixing (lower U_x) close to the injection location, consequence of the oscillating motion. This improvement decreases while moving further downstream until x/d_h=112 is reached and where both injectors present the same spatial unmixedness.

However regarding, for example, NO_x emissions in gas turbine combustors, the total mixing quality is relevant and therefore the important parameter is the total unmixedness U_t. In this respect, the fluidics technology leads to the best results, at least over the range of parameters investigated. For the momentum ratio J= 17.7, the fluidics injectors reduce the temporal unmixedness by approximately 50%. Indeed, it would potentially be possible to reduce the combustor length by 50% and still achieve the same mixing quality.

Gain in U_x and U_t

Finally, in order to summarize the findings from all the aforementioned setups, the fluidics mixing quality parameters are presented relative to the standard injection results. Figure 14 shows the ratio of the spatial unmixedness of the fluidics injection to the standard injection and Fig. 15 depicts the same ratio calculated for the temporal unmixedness. Both graphs show that the results are better close to the location of injection (i.e. at $x/d_h = 22$ in the present cases), confirming the results reported by Nathan et al. [8], and that the effect of the fluidics oscillation decreases when moving downstream. In particular, in terms of spatial unmixedness, the fluidics have a positive effect on the spatial unmixedness over a shorter distance than on the temporal unmixedness. Notably however, for small jet to crossflow momentums ($J \leq 6.4$) and high axial locations ($x/d_h \geq 50$), the reference injection presents a smaller spatial unmixedness than the fluidics set up ($U_{x,fluidics}/U_{x,ref} > 1$), though the temporal unmixedness remains lower for the latter ($U_{t,fluidics}/U_{t,ref} \leq 1$).

For both unmixedness criteria, the lowest degrees of unmixedness are achieved for the jet to crossflow momentum $J =$ 17.7, which represents then a global optimum. With this momentum ratio, the temporal mixing quality is improved by 50% across all axial locations investigated.

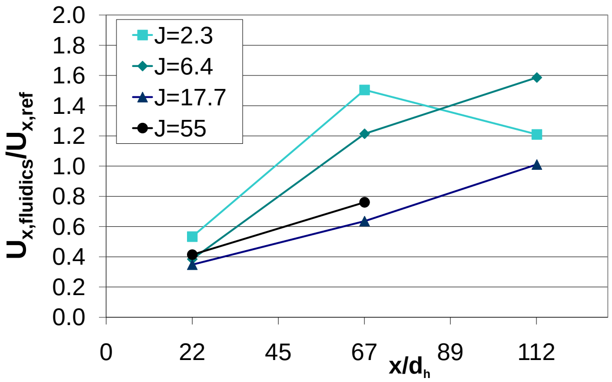

Figure 14. RELATIVE GAIN IN SPATIAL UNMIXEDNESS $U_{x,fluidics}/U_{x,ref}$ DEPENDING ON THE AXIAL LOCATION x AND FOR DIFFERENT JET TO CROSSFLOW MOMENTUMS J

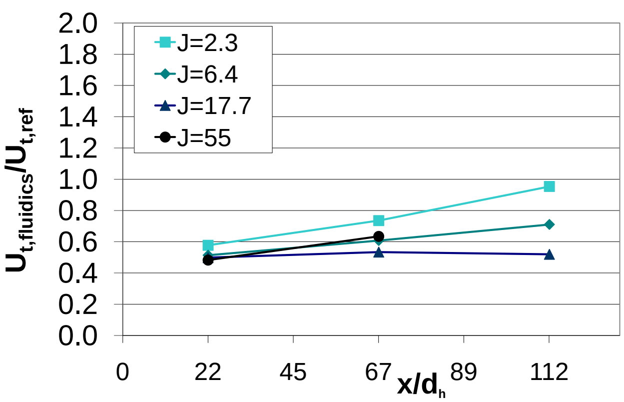

Figure 15. RELATIVE GAIN IN TEMPORAL UNMIXEDNESS $U_{t,fluidics}/U_{t,ref}$ DEPENDING ON THE AXIAL LOCATION x AND FOR DIFFERENT JET TO CROSSFLOW MOMENTUMS J

CONCLUSION

The results of this study clearly illustrate gains in terms of the mixing quality of the fluidics injection tested over a conventional jet in crossflow injection. These include:

- In all cases tested, the fluidics injectors presents the best total mixing quality U_t.
- The increase in mixing quality is higher close to the location of injection (x/d_h=22) than further downstream (x/d_h=67).
- The mixing quality of the fluidics injector is less sensitive to variations in the jet to crossflow momentum than the standard injectors.

The concentration pictures illustrate some of the effects of the fluidics injectors on the concentration field: the flapping motion distributes the dye over a wider area than the conventional jet in crossflow injectors and thus increases the macro-mixing. This increases the surface of contact of the dye jet with the surrounding flow and consequently the dilution or micro-mixing. This phenomenon appears to be the main source of improvement of the scalar mixing quality.

ACKNOWLEDGMENT

The financial support of the German Research Foundation (DFG) is greatly acknowledged. The authors would also like to thank Lars Matho and Bernhard Bobusch for their support during the measurement campaign.

REFERENCES

[1] Gutmark, E., and Grinstein, F., 1999. "Flow control with non circular jets". *Annual review of fluid mechanics,* **31**(1), pp. 239–272.

[2] Liscinsky, D. S., True, B., and Holdeman, J. D., 1995. "Crossflow mixing of noncircular jets". *AIAA Paper 95-0732*.

[3] Johari, H., Pacheco-Tougas, M., and Hermanson, J., 1999. "Penetration and mixing of fully modulated turbulent jets in crossflow". *AIAA Journal,* **37**(7), pp. 842–850.

[4] Johari, H., 2006. "Scaling of fully pulsed jets in crossflow". *AIAA journal,* **44**(11), p. 2719.

[5] Eroglu, A., and Breidenthal, R., 2001. "Structure, penetration, and mixing of pulsed jets in crossflow". *AIAA Journal,* **39**(3), pp. 417–423.

[6] Lacarelle, A., Matho, L., and Paschereit, C. O., 2010. "Sacalar mixing enhancement in a swirl stabilized combustor through passive and active injection control". *AIAA Paper 2010-1332*.

[7] Coussement, A., Gicquel, O., Schuller, T., and Degrez, G., 2010. "Large eddy simulation of pulsed jet in crossflow". *AIAA Paper 2010-561*.

[8] Nathan, G., Mi, J., Alwahabi, Z., Newbold, G., and Nobes, D., 2006. "Impacts of a jet's exit flow pattern on mixing and combustion performance". *Progress in Energy and Combustion Science,* **32**(5-6), pp. 496 – 538.

[9] Guyot, D., Paschereit, C., and Raghu, S., 2009. "Active Combustion Control Using a Fluidic Oscillator for Asymmetric Fuel Flow Modulation". *International Journal of Flow Control,* **1**(2), pp. 155–166.

[10] Danckwerts, P. V., 1952. "The definition and measurement of some characteristics of mixtures". *Appl. sci. Res., Section A, Vol. 3*, pp. 279–296.